7. Modulation of Laser Diodes*

G. Arnold, P. Russer, and K. Petermann

With 25 Figures

GaAs double-heterostructure semiconductor injection lasers which now exhibit more than 25,000 h cw room temperature lifetime are of great interest for future use as directly modulated transmitter for high bit-rate fiber optical communications. The effects limiting this application are modulation distortions, spectral width and additional spectral broadening in the case of modulation and self-pulsations of the output power. The dynamic and spectral behavior of injection lasers, the methods of high bit-rate modulation and the improvement of the high bit-rate modulation capability by coupling two lasers are discussed.

7.1 Background

Semiconductor injection lasers are of great interest as transmitters for high bit-rate fiber optical communication systems [7.2]. The main advantages of semiconductor injection lasers are simple construction, small dimensions, high efficiency and direct modulation capability up to the GHz range. Semiconductor injection lasers yield a good coupling efficiency also into monomode fibers [7.3] and for their narrow emission spectra only a low pulse broadening due to fiber dispersion when monomode fibers are used. At the wavelength of GaAs injection lasers the dispersion of usual monomode fibers is 1 ns km^{-1} for 1 % relative optical bandwidth [7.4, 5].

Considerable effort has been undertaken in recent years to develop cw lasers with long lifetimes at room temperature. Today lifetimes greater than 25,000 h have been achieved [7.6, 7]. Lifetime measurements at elevated temperatures yield extrapolated room temperature lifetimes in excess of 100 years [7.8]. Several review papers on semiconductor injection lasers have been written [7.9–13]. In this paper we shall discuss the modulation and spectral properties of double-heterostructure (DHS) stripe-geometry $GaAs/Ga_{1-x}Al_xAs$ injection lasers for cw room temperature operation. The results on these devices may be considered to be representative also for semiconductor lasers based on other materials. Especially injection lasers for longer wavelengths based on InGaAsP/InP are very attractive [7.14–17]. The dynamic behavior of these devices is very similar to that of GaAs lasers, as reported in [7.18, 19].

* Expanded and updated treatment based upon a paper published in Appl. Phys. [7.1].

For high bit-rate communication from several 100 Mbit/s up into the Gbit/s range, lasers must have the following properties:

i) No modulation distortions (pattern effects);
ii) A narrow spectral bandwidth;
iii) No high spectral broadening due to direct modulation;
iv) No self-pulsations.

The rate equations which describe the dynamic behavior of injection lasers are discussed in detail in Sect. 7.2. In the following sections we review and discuss the modulation, spectral and self-pulsation behavior of injection lasers, and the methods for direct modulation at high bit rates.

7.2 The Rate Equations

Semiconductor injection lasers exhibit a very complex dynamic behavior. Until now, not all experimentally observed effects can be explained satisfactorily; but for the main properties, a good theoretical understanding has been achieved. The dynamics of a semiconductor injection laser is governed by rate equations [7.20–27]. The quantum-mechanical rate equations for the electron density and polarization operators and the photon amplitude operators give information about the time development of the photon amplitude, frequency and phase and also about the statistical properties due to quantum fluctuations [7.20, 23, 24, 26]. In many cases, where only the time dependence of the photon number mean value is of interest and an interaction of modes with a very narrow wavelength spacing does not occur, the analysis can be performed by the much simpler classical rate equations for the electron density in the active layer and the photon numbers in the modes [7.21, 22, 25, 27]. Due to the intraband scattering processes spectral hole burning is unimportant in injection lasers and the cause for the mainly observed multimode operation of injection lasers is assumed to be spatial hole burning [7.28–31]. We give multimode rate equations for the electron density and photon numbers. In the multimode case the inhomogeneous distribution of electron and photon densities must be taken into account. For an active layer, parallel to the $x-y$ plane with a thickness d, these rate equations are

$$\frac{\partial n(x,y,t)}{\partial t} = \frac{J(x,y,t)}{e_0 d} - \frac{1}{\varkappa} R_{sp}(n) + D\nabla^2 n(x,y,t) - \frac{1}{d}\sum_i \frac{\Gamma_i}{\Phi(E_i)} S_i(t)|\varphi_i(x,y)|^2 r_{st}(E_i,n), \tag{7.1}$$

$$\frac{\partial S_i(t)}{\partial t} = -\frac{S_i(t)}{\tau_{ph_i}} + \frac{\Gamma_i}{\Phi(E_i)} \int |\varphi_i(x,y)|^2 r_{sp}(E_i,n)\,dx\,dy + \frac{\Gamma_i}{\Phi(E_i)} S_i(t) \int |\varphi_i(x,y)|^2 r_{st}(E_i,n)\,dx\,dy. \tag{7.2}$$

The electron density n depends on x and y and is assumed to be confined within the active layer and constant therein in z direction. J is the injection current density, e_0 the absolute value of the electron charge. S_i is the photon number in the ith mode, $\varphi_i(x, y)$ is the normalized scalar complex photon amplitude function. The complex amplitude function is normalized so that $|\varphi_i(x, y)|^2$ integrated over the whole $x-y$ plane yields 1. Γ_i is the photon confinement factor which gives the ratio of photon energy concentrated within the active layer of volume V to the total photon energy, both for the ith mode [7.13]. The stimulated and spontaneous emission rates per unit of volume and unit of photon energy r_{st} and r_{sp} have been calculated by *Lasher* and *Stern* [7.32] for GaAs at room temperature, assuming transitions between parabolic bands with k selection rule for pure material and without k selection rule for highly doped material. For parabolic bands without k selection rule, and additional Gaussian impurity band tails calculations have been performed by *Casey* and *Stern* [7.33]. For transitions between parabolic bands without k selection rule an approximate expression for r_{st} has been given by *Marinelli* [7.34]. R_{sp} is the total spontaneous emission rate per unit of volume, and $\varkappa$ is the internal quantum efficiency. $\Phi(E_i)$ is the number of modes per unit of volume and unit of energy and is given by

$$\Phi(E_i) = \frac{\bar{n}_i' \bar{n}_i^2 E_i^2}{\pi^2 \hbar^3 c^3}, \tag{7.3}$$

where $\bar{n}_i$ is the index of refraction for the ith mode, and the effective index of refraction $\bar{n}_i'$ considering the dispersion is given by

$$\bar{n}_i' = \bar{n}_i \left(1 - \frac{\lambda_i}{\bar{n}_i} \frac{d\bar{n}_i}{d\lambda_i}\right). \tag{7.4}$$

For a vacuum wavelength of 8500 Å we obtain $E_i = 1.46\,\text{eV}$ and with $\bar{n} = 3.6$ and $\bar{n}' \approx 5$ [7.35] the number of modes per unit of volume and unit of energy is $\Phi(E_i) = 1.817 \times 10^{12}\,\text{meV}^{-1}\,\text{cm}^{-3}$. D is the diffusion constant and can be calculated from $D = \mu_n kT/e_0$ (where μ_n is the electron mobility, k the Boltzmann constant and T the absolute temperature) or from $D = L_n^2/\tau_{sp}$ (where τ_{sp} is the spontaneous electron lifetime and L_n the electron diffusion length). From $\mu_n = 3000\,\text{cm}^2\,\text{V}^{-1}\,\text{s}^{-1}$ for GaAs and $kT/e_0 = 26\,\text{mV}$ the electron diffusion constant $D_n = 78\,\text{cm}^2\,\text{s}^{-1}$ for p-doped GaAs is calculated. This value coincides well with the result calculated from $L_n = 5\,\mu\text{m}$ for Ge-doped p-type GaAs layers [7.36] and $\tau_{sp} = 3\,\text{ns}$. In highly doped GaAs, the minority carrier diffusion constant can be smaller by more than an order of magnitude [7.28, 30]. The photon lifetime τ_{ph_i} in the ith mode is given by [7.25]

$$\tau_{ph_i}^{-1} = \frac{c}{\bar{n}_i'} \left(\alpha_i' - \frac{1}{L} \ln R_i\right), \tag{7.5}$$

where α_i' is the internal optical loss per unit length, R_i the reflectivity of the end mirrors, both for the ith mode and L is the laser length. For solution grown junctions at room temperature the photon lifetimes are between 1 and 2 ps [7.37].

The computational analysis of the single-mode laser in many cases yields considerable insight into the laser dynamics. To some extent the results are also applicable to the physically more realistic multimode case. If only one mode oscillates, hole burning effects can be neglected and the spatial distribution of the electron and photon densities can be considered uniform within the active region. In this case the summation in (7.1) over i has to be deleted and $d^{-1}|\varphi(x,y)|^2$ has to be substituted by V^{-1}, in (7.2) the integrals over $|\varphi(x,y)|^2$ have to be replaced by 1. A further simplification of the monomode rate equations is possible by the following approximations

$$\varkappa^{-1} R_{sp}(n) \approx n/\tau_{sp}, \tag{7.6}$$

$$\frac{\Gamma}{\Phi(E_s)} r_{sp}(E_s, n) \approx \frac{\alpha V n}{\tau_{sp}}. \tag{7.7}$$

Measured spontaneous electron lifetimes τ_{sp} of DHS lasers at room temperature are between 2 and 8 ns [7.18, 38, 39]. The coefficient α, defined by (7.6, 7) gives the ratio of the spontaneous emission rate into the oscillating mode to the total spontaneous electron recombination rate. To give a rough estimate of the maximum value of α we set the internal quantum efficiency $\varkappa = 1$ and $R_{sp}(n)$ equal $r_{sp}(E_s, n)$ times the spontaneous emission linewidth. For $V/\Gamma = 10^{-9}\,\mathrm{cm}^3$, a spontaneous emission linewidth of 300 Å, and for the above calculated $\Phi(E_s) = 1.817 \times 10^{12}\,\mathrm{meV}^{-1}\,\mathrm{cm}^{-3}$ we obtain $\alpha = 1.07 \times 10^{-5}$. On the basis of Marinelli's approximation formula, *Adams* has proposed a similar approximation for the stimulated emission coefficient

$$\frac{\Gamma}{V\Phi(E_s)} r_{st}(E_s, n) = g n^l, \tag{7.8}$$

where $l = 3$ for GaAs double-heterostructure lasers at room temperature [7.27]. These approximations yield the rate equations

$$\frac{dn}{dt} = \frac{J}{e_0 d} - \frac{n}{\tau_{sp}} - g S n^l, \tag{7.9}$$

$$\frac{dS}{dt} = -\frac{S}{\tau_{ph}} + \alpha V \frac{n}{\tau_{sp}} + V g S n^l. \tag{7.10}$$

For $\alpha=0$ and $J \geqq J_{th}$ the explicit solution of the steady-state rate equations is

$$n_{th}=\left(\frac{1}{Vg\tau_{ph}}\right)^{1/l}, \tag{7.11}$$

$$S=V\frac{\tau_{ph}}{\tau_{sp}}\left(\frac{1}{Vg\tau_{ph}}\right)^{1/l}(J/J_{th}-1), \tag{7.12}$$

where n_{th} is the threshold electron density at which the gain in the active region compensates the resonator losses. The threshold current density J_{th} is given by

$$J_{th}=e_0 d n_{th}/\tau_{sp}. \tag{7.13}$$

Figure 7.1 shows the experimental light output vs current characteristics of two different injection lasers. Laser 1 shows a linear slope above threshold. The slope below threshold results from the spontaneous emission with a broad spectral distribution. The nonlinearity in curve 2 will be discussed later.

7.3 Direct Modulation of Injection Lasers

If a step current pulse of amplitude I (the injection current I is given by the product of the injection current density J and the junction area) is applied to the laser, an initial delay time t_d passes until the onset of the laser oscillations and then the coherent emission starts with relaxation oscillations in the output power [7.40, 41]. The transient solution of the rate equations has been given by several authors [7.27, 42–45].

Figure 7.2a shows the transient response of a monomode injection laser to a step current pulse. We use the normalized electron density $z=n/n_{th}$, the normalized photon number $x=S\tau_{sp}/Vn_{th}\tau_{ph}$ and the normalized injection current $\eta=I/I_{th}=J/J_{th}$. The laser parameters are $\tau_{sp}\tau_{ph}=10^3$, $l=3$, $\alpha=2\times10^{-5}$. The normalized step current pulse amplitude is $\eta=1.1$. If a step current pulse of amplitude I is applied to an initially unbiased injection laser, the electron density in the active layer increases. As long as n is well below n_{th} no considerable amplification of the spontaneously emitted photons takes place. After the initial delay time [7.40, 41]

$$t_d=\tau_{sp}\ln\left[I/(I-I_{th})\right] \tag{7.14}$$

the electron density in the active layer reaches its threshold value and the photon number rises fast. As long as the photon number is below its stationary value, the electron density further increases above n_{th}. When S passes its stationary value, due to the rapidly increasing stimulated recombination processes, the electron density quickly decreases but the photon number further

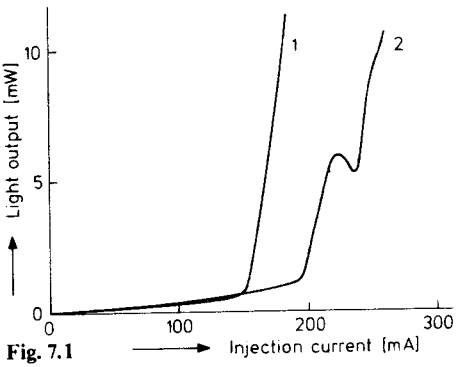

Fig. 7.1

Fig. 7.1. Experimental light output vs current characteristics for two different injection lasers

Fig. 7.2a–c. Transient response of an injection laser to a step current pulse for different spontaneous emission contributions

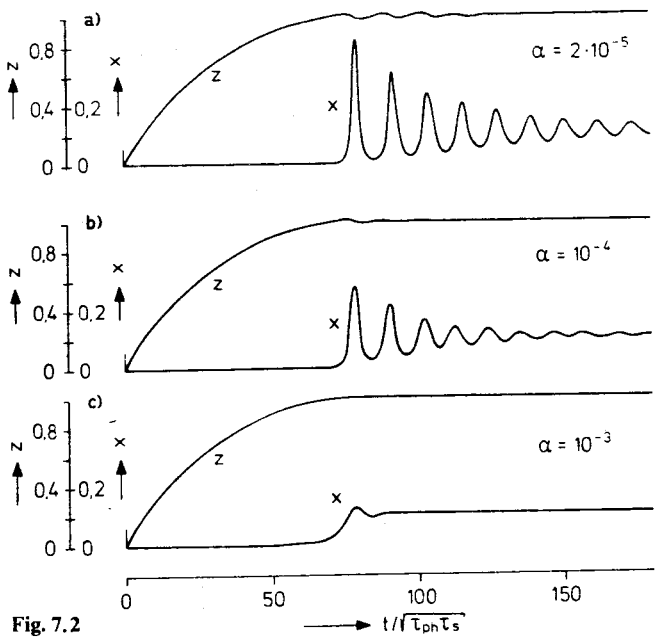

Fig. 7.2

increases until n passes again n_{th}. The fast decrease of the electron density continues until the photon number falls below its stationary value. If the amplitude of the first photon spike is much higher than the stationary photon number, a considerable decrease of n below n_{th} during the decrease of the light pulse takes place. Since the electron density is slowly raised again the photon number may decrease by several orders of magnitude until n has again reached n_{th}. Afterwards the whole process is repeated, but since the photon number in the considered mode now is higher than at the beginning of the process when n passed n_{th}, the photon number reaches its equilibrium value at a shorter time. Therefore the overshoot in the electron density and the following

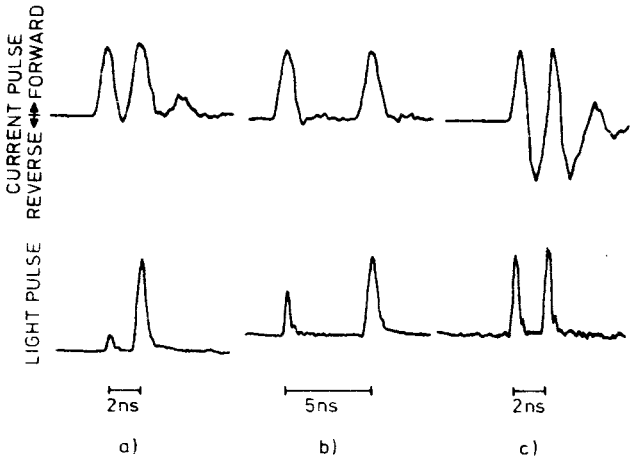

Fig. 7.3. Current pulse (upper trace) and corresponding light pulse (lower trace) of a GaAs GaAlAs DHS stripe-geometry laser operated with double pulses with different pulse spacing (**a**) 2 ns, (**b**) 5 ns, and (**c**) 2 ns with pulses of forward and reverse swings [7.48]

photon number overshoot are smaller than before. The process is repeated until the stationary state is reached.

For pulse modulation applications of injection lasers the delay time can easily be reduced by prebiasing the laser with a dc current I_0 [7.44, 46]. When a current pulse with amplitude I_p is superimposed the delay time is

$$t_d = \tau_{sp} \ln[I_p/(I_p - I_{th} + I_0)]. \tag{7.15}$$

If the laser is biased up to threshold, t_d vanishes. If the laser is unbiased or biased below threshold and modulated with two subsequent pulses the delay time for the second pulse is reduced [7.40] since the electron density after the first current pulse is higher than before. In the case of direct pulse code modulation this would cause a pattern effect. *Ozeki* and *Ito* suggested the modulation of the injection laser by an additional compensation pulse before each modulation pulse which is preceded by a logical zero [7.47]. This compensation pulse is too small to generate a light pulse but raises the electron density up to the same level as a foregoing modulation pulse would have done. Two similar methods for pattern effect reduction have been shown by *Lee* and *Derosier* [7.48]. In the first case, the modulation pulse amplitude is dependent on whether a modulation pulse preceded or not. In the second case the modulation signal consists of double pulses with a forward and a reverse swing (Fig. 7.3). The first forward swing causes the light pulse, whereas the second negative swing removes the excess charge in the active region. For prebiasing near threshold a pulse spacing of 2 ns is achieved without pattern effect.

With increasing contribution of spontaneous emission into the oscillating modes, the damping of the relaxation oscillations is raised since the initial photon number in that case is higher, the stationary photon number is reached earlier and the overshoot consequently is smaller [7.43, 45, 49]. In the multimode case the relative contribution of spontaneous emission into the oscillating modes is proportional to the number of oscillating modes when the monomode calculation is taken as representative for the photon number in all oscillating modes. Figure 7.2b, c shows calculations of the transient behavior with $\alpha = 10^{-4}$ and $\alpha = 10^{-3}$. *Angerstein* and *Siemsen* deduced from measurements on DHS stripe-geometry injection lasers α as high as 5×10^{-4} [7.39]. Values of $10^{-3} < \alpha < 10^{-2}$ fitted to measurements on buried heterostructure lasers cannot be explained by such a strong spontaneous emission [7.50]. Pulse code modulation of injection lasers has been achieved up to more than 2 Gbit/s [7.51–56]. Figure 7.4 shows the direct modulation of an injection laser at 2.3 Gbit/s. Figure 7.5 shows the result of a 280 Mbit/s modulation experiment with a low mesa-stripe DHS injection laser [7.56]. When the laser is biased below threshold the light output shows a strong pattern effect. If the laser is biased 5% above threshold the pattern effect vanishes but the laser output exhibits a strong ringing, since every modulation pulse causes relaxation oscillations. We have seen that in the case of biasing below threshold pattern effects arise from the electron density dependence on a preceding pulse. In the case of biasing the laser above threshold the optical output pulse not only depends on the initial electron density in the active layer but also on the initial photon number in the oscillating modes. *Danielsen* has suggested avoiding the pattern effects in Gbit/s PCM by biasing the laser approximately to threshold and giving the height and duration of the applied current pulses such values that the laser only emits the first spike of the relaxation oscillations and the electron and photon densities at the end of the current pulse return to their initial values [7.57]. In many experiments, we have seen that in the case of pulse code modulation above 250 Mbit/s, when the laser is biased near threshold an exact adjustment of the bias current and the modulation amplitude is necessary. This can be well explained by the theory of *Danielsen*.

Sinusoidal modulation of injection lasers above threshold is a powerful tool for investigating the dynamic properties of injection lasers. Small-signal analysis yields a resonance in the modulation depths vs modulation frequency curve [7.27, 58–60]. If I_1 is the complex modulation current amplitude and S_1 the complex photon number amplitude, both at the angular frequency ω, and if the laser is biased to I_0 and S_0, respectively, we obtain by small-signal analysis of the rate equations (7.9, 10) for $\alpha = 0$

$$S_1/S_0 = (l/\tau_{sp}\tau_{ph}) \frac{I_1/I_0}{\omega_0^2 + j\omega\beta - \omega^2} \tag{7.16}$$

with

$$\omega_0^2 \tau_{sp}\tau_{ph} = l(I\ I_{th} - 1) \tag{7.17}$$

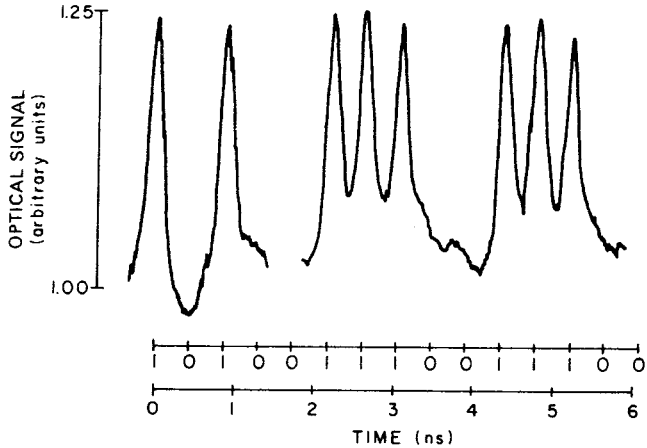

Fig. 7.4. Direct modulation of an injection laser at 2.3 Gbit/s

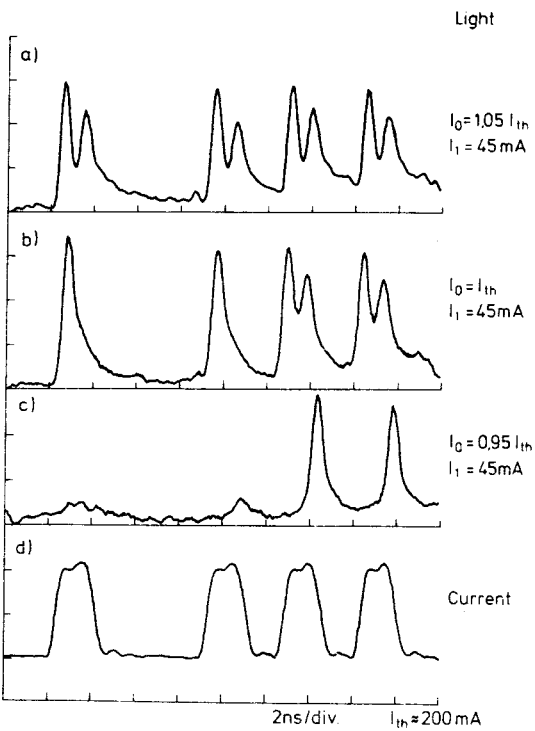

Fig. 7.5a–d. Direct modulation of an injection laser at 280 Gbit/s and different bias currents

and

$$\beta\tau_{sp} = I(I/I_{th} - 1) + 1 . \tag{7.18}$$

Small-signal calculations including the effect of spontaneous emission have been performed by *Harth* and *Siemsen* [7.49]. Figure 7.6 shows the dependence

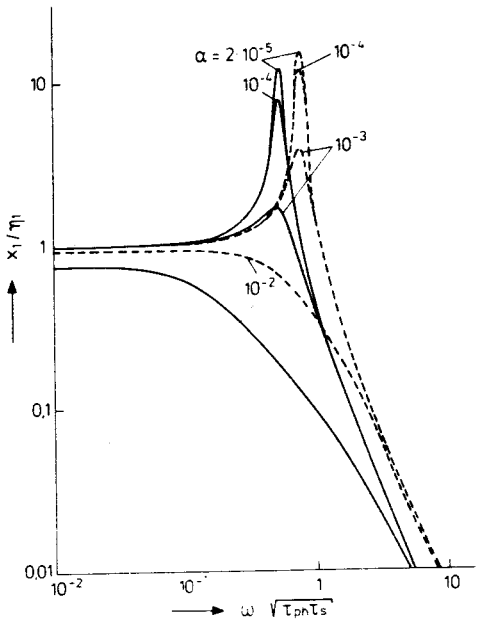

Fig. 7.6. Small-signal modulation depths dependence on modulation frequency for biasing 10% (continuous curve) and 20% (broken curve) above threshold for τ_{sp}, $\tau_{ph} = 10^3$ and different α

of modulation depths on the modulation frequency for biasing 10 and 20%, respectively, above threshold calculated from (7.9, 10) for $l = 3$ and $\alpha = 2 \times 10^{-5}$, 10^{-4}, 10^{-3}, 10^{-2}. The last two values of α are possible only in the case of many excited modes. The results of the small-signal analysis suggest that a biasing of the injection laser much above threshold would be preferable for high-frequency modulation. Unfortunately, the laser there exhibits irregular phenomena which we shall discuss in Sects. 7.5, 6. Furthermore, for optical communication applications a high dc light power level would also raise the shot noise in the receiver. The use of multimode lasers with a higher α is in contradiction with the narrow bandwidth requirements for low fiber dispersion.

When the laser is modulated by large sinusoidal currents the resonance frequency can be reduced considerably and the light output signal becomes distorted [7.61, 62]. With $l = 1$ and $\alpha = 0$ in (7.9, 10) according to [7.62] the analytical expression for the time dependence of the photon density is

$$S(t) = \frac{S_0}{\tilde{I}_0(a)} \exp[a \cos(\omega t + \theta)], \tag{7.19}$$

where $\tilde{I}_0(a)$ is the modified Bessel function of the first kind and of order zero, and a is an amplitude factor depicted in Fig. 7.7. At the large-signal resonance frequency where $a \gg 1$ from (7.19) a pulse-like shape of the optical output signal arises (Fig. 7.8). We emphasize that this strong nonlinearity occurs although a completely linear dc light output vs current characteristic is assumed. This imposes restrictions on the application of amplitude modulation for high

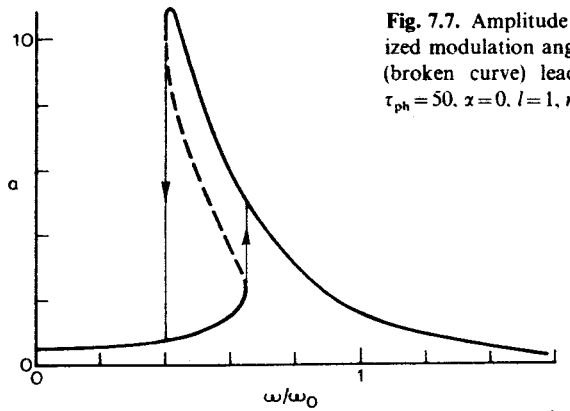

Fig. 7.7. Amplitude factor a as a function of the normalized modulation angular frequency. An unstable region (broken curve) leads to hysteresis phenomena (τ_{sp}, $\tau_{ph}=50$, $\alpha=0$, $l=1$, $\eta_0=1.5$, $\eta_1=0.5$) [7.62]

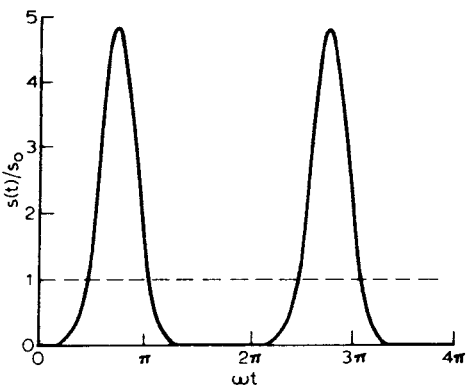

Fig. 7.8. Normalized photon density as a function of time [7.62]

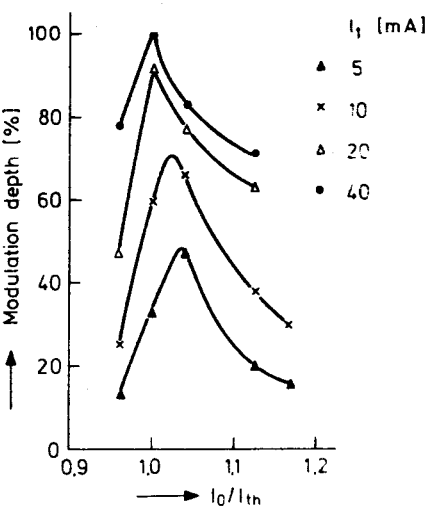

Fig. 7.9. Modulation depth as a function of the bias current I_0 for 280 MHz sinusoidal modulation at different modulation amplitudes I_1

bandwidth fiber communication systems. The amplitude factor a has a maximum at threshold for which it yields a maximum modulation depth. Our experimental investigations of the large-signal modulation depth as a function of the normalized bias current I_0/I_{th} confirm these theoretical results (Fig. 7.9). By generating spikes with a small sinusoidal current at the modulation resonance frequency and removing one or more light pulses by a short lowering of the bias, *Schicketanz* has demonstrated pulse code modulation at 650 Mbit/s [7.54]. Further investigations of the nonlinear rate equations have shown that by modulation at the double resonance frequency also subharmonics can be excited [7.63] and the small-signal modulation sensitivity can be increased by an additional large sinusoidal modulation current [7.64, 65].

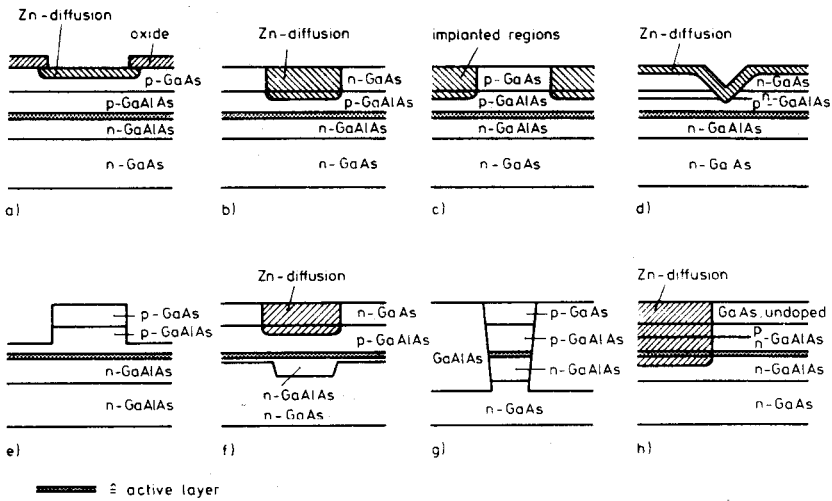

Fig. 7.10a–h. Several laser structures. (**a**) Oxide-stripe laser; (**b**) Diffused-stripe laser; (**c**) Proton-implanted laser; (**d**) *V*-groove laser; (**e**) Low-mesa-stripe laser; (**f**) Channelled-substrate-planar (CSP) laser; (**g**) Buried-heterostructure (BH) laser; (**h**) Transverse-junction-stripe (TJS) laser

7.4 Modulation Behavior of Specific Laser Structures

In the preceding section, the modulation behavior of injection lasers has been discussed in general without referring to special laser structures. In recent years a large number of proposals for specific laser structures has been made. We shall now direct our attention to the correlations between geometry and the dynamic properties of injection lasers.

Some of these structures are shown in Fig. 7.10. It is convenient to relate the large variety of laser structures to the following subgroups which differ mainly in the mode-guiding mechanism and the mode volume of the lasing modes:

i) Injection lasers with no built-in index waveguide. The lasing mode in these lasers is guided only by the gain profile due to the current injection from the stripe contact. Especially the oxide-stripe laser (Fig. 7.10a), the diffused-stripe laser (Fig. 7.10b) with shallow diffusion, the proton-implanted laser (Fig. 7.10c) and the *V*-groove laser [7.66] (Fig. 7.10d) belong to that group. The gain-guiding mechanism also predominates in the low-mesa-stripe laser [7.67] (Fig. 7.10e), as long as a broad mesa structure with a stripe width in excess of about 15 μm is used.

ii) Injection lasers with a built-in index waveguide. Improved laser characteristics are expected if the lasing mode is guided by a stable built-in waveguide. In order to have efficient waveguiding the built-in waveguide should be sufficiently narrow so that a gain-guided mode with self-focusing properties [7.68] cannot develop. The CSP laser [7.69] (Fig. 7.10f) and the diffused-stripe

laser with deep diffusion [7.70] are examples, belonging to the second group. In addition, the buried-heterostructure (BH) laser [7.71] (Fig. 7.10g) also exhibits a stable built-in waveguide.

iii) Lasers with very small transverse dimensions of the active layer. Examples of this third group are represented by the BH laser as mentioned above and by the transverse-junction-stripe laser [7.72] (Fig. 7.10h).

The laser groups mentioned above differ in their modulation behavior. These differences are introduced on the one hand by the different ratios α of the spontaneous emission into the lasing modes, as discussed in the preceding section. On the other hand, diffusion processes within the active layer and dynamic interactions with higher order modes also play an important role in the modulation behavior [7.30, 73, 74].

Let us begin the discussion by considering planar-stripe lasers according to the laser subgroup (i). Since the waveguide for the lasing modes is accomplished here mainly by the gain distribution as introduced by the injected carriers, any dynamic change of the carrier distribution also introduces a change in the waveguiding properties. An accurate description of the modulation behavior of planar-stripe lasers therefore requires numerical calculations [7.73].

If the width of the injected carriers in such lasers exceeds the width of the fundamental mode field, deformations of the spatial gain profile (hole burning) may occur so that eventually a first-order mode is created during the modulation. An example of that kind will be discussed in the next section. Improved modulation characteristics are therefore obtained, if transverse spatial hole burning is avoided. This can be done by lowering the stripe width of lasers down to the order of 2 to 3 μm [7.75]. Such a small stripe width can also be easily achieved when using the *V*-groove structure [7.66] according to Fig. 7.10d. The width of the fundamental lasing mode is then in the same order as the width of the injected current or even larger. Therefore hole-burning effects are less probable to occur. In addition, the diffusion length comes into the same order of magnitude as the modal width. Diffusion effects then yield a reduction of the relaxation oscillations as calculated in [7.74]. Experimentally, very narrow stripe lasers therefore show no relaxation oscillations [7.75], which is also caused by the larger value of the spontaneous emission coefficient α due to the small active volume according to (7.7).

Diffusion processes yield a significant reduction of relaxation oscillations for lasers of the subgroup (ii) if the width of the built-in waveguide is in the order of the diffusion length or even smaller. A reduction of relaxation oscillations especially occurs if the transverse current injection extends beyond the built-in waveguide since then carriers from outside may diffuse into the region of the oscillating mode yielding a reduction of relaxation oscillations [7.73]. Such a behavior has been theoretically calculated and is found to be in good agreement with experimental observations on CSP lasers [7.73].

In the laser subgroup (iii) the transverse width of the active layer is reduced down to 1 to 2 μm. For the case of lateral carrier confinement and an active layer width considerably smaller than the diffusion length, the shape of the gain

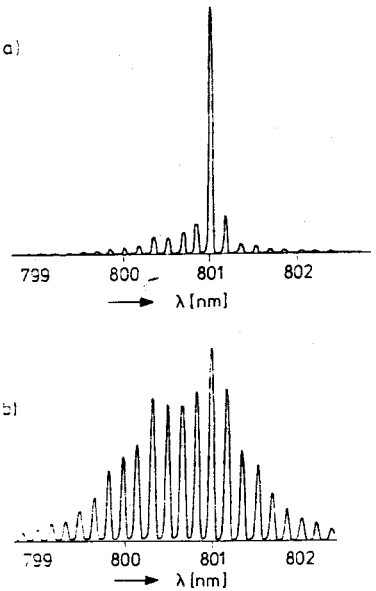

Fig. 7.11a, b. Emission spectrum of a low-mesa-stripe GaAs DHS injection laser 3% above threshold (**a**) and close to threshold (**b**)

profile is only weakly influenced by diffusion processes. *Suematsu* et al. [7.74], and *Chinone* et al. [7.73] have calculated that, therefore, no significant diffusion-induced reduction of the resonance peak of the relaxation oscillations occurs in this case. The case of lateral carrier confinement in connection with low stripe width is realized by the BH laser [7.71]. Due to the small volume V of the active layer (7.7) yields a large spontaneous emission coefficient yielding a stronger reduction of the relaxation oscillations. A nearly flat frequency response for frequencies up to 2 GHz has been reported for BH lasers [7.71]. TJS lasers have also a small volume of the active layer but differ from the BH laser in that the carriers are not strictly confined. TJS lasers were shown to exhibit only a small pattern effect when modulated with a 400 Mbit/s PCM signal [7.76].

7.5 Effect of Modulation on Spectrum and Near Field

The dc spectral [7.10, 13, 35, 77] and near field [7.13, 78–80] behavior of injection lasers have been widely discussed. We have investigated the influence of modulation on the emission properties of injection lasers. Far below threshold, injection lasers exhibit a broad spontaneous emission spectrum (approximately 300 Å) which is narrowed with increasing current and exhibits a mode structure at and above threshold (Fig. 7.11). The laser can oscillate in a single or in a number of transverse modes and also in one or more filaments.

The tendency to more filaments or to higher-order transverse modes increases with the stripe width of the active region and with the pumping above threshold. The latter increase is due to transverse spatial hole burning [7.30]. Each filament or transverse mode exhibits a longitudinal mode group. Since the gain spectrum of injection lasers has a broad maximum, also very small longitudinal hole burning should yield a number of longitudinal modes within the same transverse mode family. The envelopes of the longitudinal mode groups can be different in wavelength and intensity of the maximum. For the longitudinal modes the wavelength separation $\Delta\lambda$ of adjacent modes can be calculated from [7.35]

$$\Delta\lambda = \frac{\lambda_i^2}{2Ln_i'}. \tag{7.20}$$

For a typical laser length of 200–400 μm the longitudinal modes are separated by 1.5–3 Å. The transverse modes along the junction plane, however, have a separation in the order of 0.1 Å [7.10]. The spectral position of these lasing modes is very sensitive to temperature changes owing to two effects [7.13]. First, the band gap of a semiconductor decreases with increasing temperature. As a result the wavelength of the laser emission increases with temperature. This temperature coefficient is approximately 2.5 Å/K. The wavelength of an individual spectral mode has a temperature coefficient of approximately 0.4 Å/K because of the temperature dependence of the refractive index of the semiconductor [7.81]. To observe narrow spectral lines a careful temperature control of the laser is necessary. The temperature effects can influence the emission spectrum if the temperature of the junction region of the laser is increased in the course of the modulation pulse duration.

Many stripe-geometry DHS GaAs/GaAlAs lasers show nonlinearities – the so-called kinks – in the light output vs current characteristics [7.80, 82, 83]. Laser 2 in Fig. 7.1 shows a typical kink in the light output characteristic of a low-mesa-stripe DHS injection laser with stripe width 25 μm. It has been found that these kinks are associated with filamentary structures of the near-field intensity distribution parallel to the junction plane, spatial movement of the filaments within the stripe width, and excessive spectral broadening of the emission spectrum. Moreover, the location and character of the kinks can change during longtime operation of lasers. Recently, *Dixon* et al. [7.83] reported an improved linear light output vs current characteristic by reducing the excited stripe width of the active region of the DHS GaAlAs lasers below 10 μm, whereas almost all lasers with a stripe width ranging from 10–20 μm show kinks [7.84]. In narrow stripe lasers the kinks move to a higher current range and may occur again at higher light output power.

Experimental and theoretical investigations show that high-frequency direct modulation causes an intensity decrease of dominant modes while the number of neighboring longitudinal modes is increased. Consequently, the spectral envelope is broadened [7.85–88]. When the injection current is

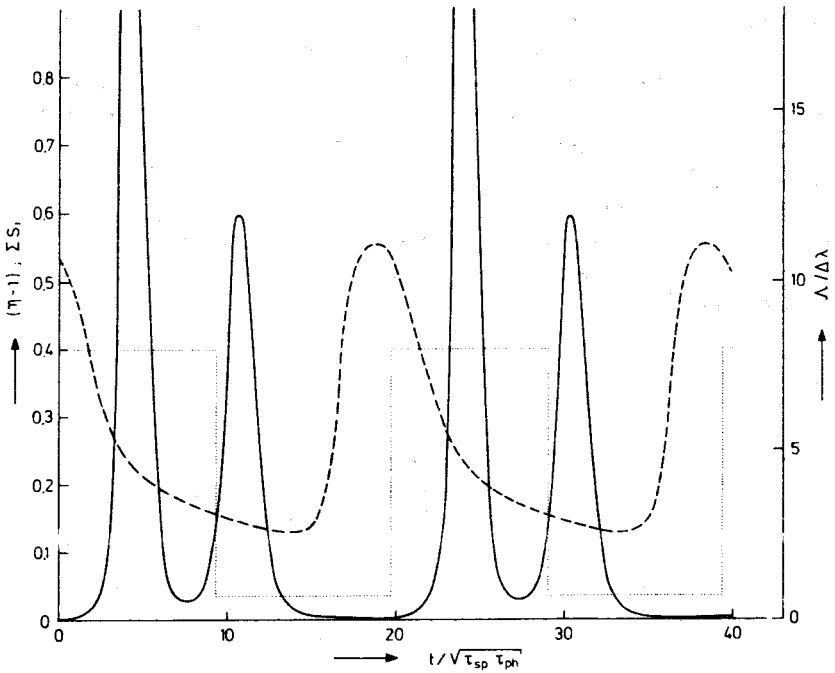

Fig. 7.12. Response to a modulation with rectangular current pulses: (····) injection current; (———) photon density; (----) spectral halfwidth

modulated, the electron density also oscillates with the modulation frequency. The electron density modulation amplitude increases with the modulation current amplitude and also with the modulation frequency. If the electron density oscillates there are periods when modes with a higher threshold electron density may have a net gain and the number of oscillating modes is increased.

Figure 7.12 shows a theoretical calculation of the photon response and the temporal development of the spectral emission halfwidth by use of the multimode rate equations, if the laser is operated with rectangular pulses which change the injection current from 3.5% above threshold to 40% above threshold [7.88]. The spectral halfwidth Λ is normalized with respect to the mode spacing $\Delta\lambda$. Though the stationary spectral width in this specific example at 3.5% above threshold is only $\Lambda = 1.6\Delta\lambda$ and decreases with increasing current, the spectral width during modulation becomes much broader. The spectral broadening just occurs during the time interval of small photon density. As soon as the photon density increases the spectral width decreases only slowly so that a relatively broad spectrum is maintained during the light pulses.

Figure 7.13 shows the effect of 300 Mbit/s pulse code modulation on the emission spectrum of a GaAs low-mesa-stripe DHS injection laser. The quasi single-mode emission of the laser without modulation changes with increasing modulation current to a multimode emission. Besides the increase of the number of longitudinal modes, a new mode family appears.

For the interpretation of the spectral change, the modulation influenced emission spectrum has been investigated spatially and time resolved. Figure 7.14a shows the integral intensity distribution of the near field along the junction plane and Fig. 7.14b the corresponding monochromatic near-field distributions of neighboring modes belonging to different longitudinal mode families. The near-field distribution *A* belongs to the fundamental transverse mode and the intensity distribution *B*/*C* exhibits the first-order transverse mode. The spatially resolved emission spectra at the near-field positions *A*, *B*, and *C* are shown in Fig. 7.15 together with the integral emission spectrum. As can be seen, the fundamental transverse mode (*A*) yields a quasi single-mode emission spectrum which is essentially the same as the spectrum without modulation (Fig. 7.13). At the positions *B* and *C* of the first-order transverse mode an identical spectrum is measured, but it is different from the spectrum at position *A*. The peak wavelength is 4.5 Å shorter than in the spectrum of the fundamental transverse mode. The lower wavelength for the first-order mode is in agreement with the measurements of *Buus* et al. [7.30] and in contradiction to their theoretical considerations. The wavelength shift can probably be explained by higher bandfilling caused by the modulation current pulses.

In order to investigate the dynamic behavior of the emission of the modulated laser, the time resolved light pulses have been measured. In Fig. 7.16 the light pulses of the five figures "1" of the word 1000110001111100 at 300 Mbit/s are shown for the same modulation conditions as for the spatially resolved spectra. Besides the light pulses for the overall intensity distribution also the light pulses for the fundamental (*A*) and first-order (*B*, *C*) transverse modes are measured. The light pulses show spikes caused by relaxation oscillations. The first spike of the relaxation oscillations is lasing in the fundamental mode (*A*) in agreement with the results of [7.30]. The first-order transverse mode (*B*, *C*) is excited later, as can be seen from Fig. 7.16. Measurements of the time resolved spectra have yielded essentially the quasi single-mode emission spectrum of Fig. 7.13 in the first spike of the light pulse and the modulation induced spectrum with the shorter peak wavelength exhibited by the first-order mode is observed in the following spikes of the light pulse. The results of these investigations show that for certain modulation conditions it may be possible to retain the emission spectrum unchanged in spite of direct modulation of the laser, provided that the modulation pulses are very short or the light pulse is suppressed after the first spike of the relaxation oscillation. By appropriate choice of pulse amplitude and duration direct Gbit/s modulation free of pattern effects and spectral broadening is possible [7.89, 90]. However, the need of an accurate bias and pulse amplitude control would complicate technical applications of this method.

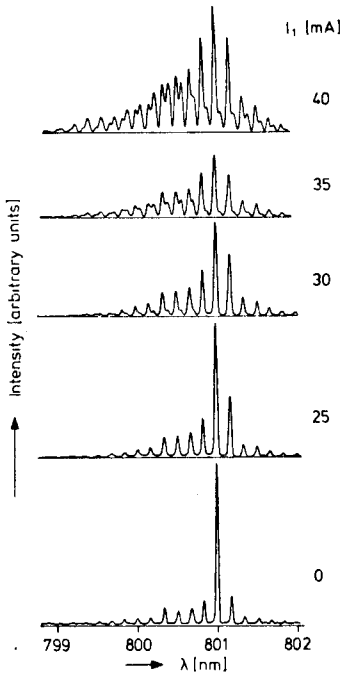

Fig. 7.13. Emission spectra of a GaAs laser directly modulated with the word 1000110001111100 at 300 Mbit /s and varying modulation current amplitude I_1. Bias current $I_0 = 130$ mA (1.02 I_{th})

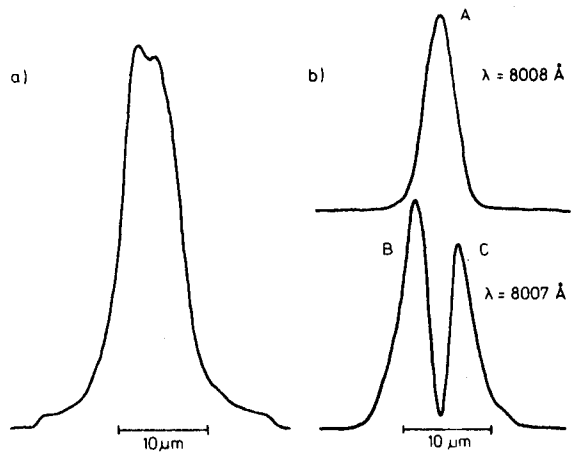

Fig. 7.14a, b. Near-field intensity distribution along the junction plane of a GaAs laser operated with 300 Mbit/s PCM. Bias current $I_0 = 130$ mA, modulation current amplitude $I_1 = 40$ mA; (**a**) total near field; (**b**) monochromatic near fields

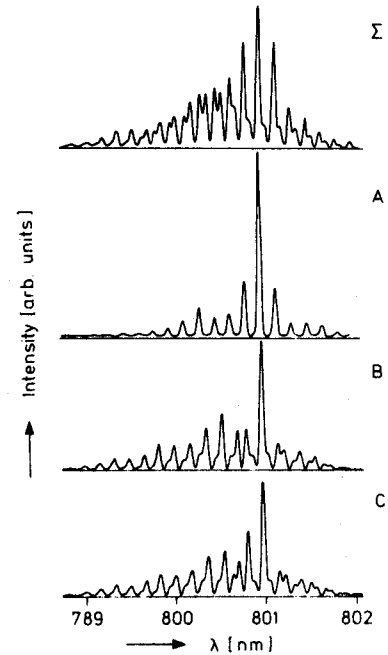

Fig. 7.15. Spatially resolved emission spectra of the GaAs laser operated as in Fig. 7.14. (Σ) Emission spectrum of the total light output; (A) emission spectrum of the fundamental transverse mode, and (B, C) emission spectrum of the first-order transverse mode

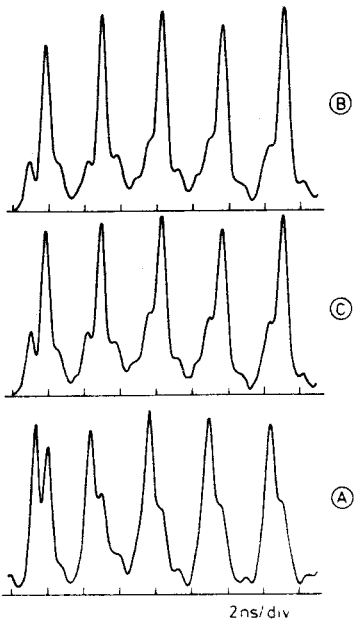

Fig. 7.16. Time resolved light output of the laser operated as in Fig. 7.14. Light pulses of the five "1" of the word 1000110001111100. Ⓐ Light pulses in the fundamental transverse mode, and Ⓑ, Ⓒ light pulses in the first-order mode

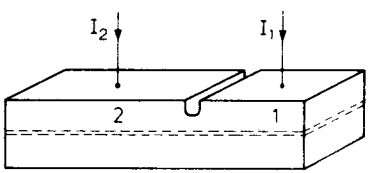

Fig. 7.17. Double section injection laser

7.6 Self-Pulsing Phenomena

From (7.17, 18) can be seen that the modulation bandwidth of injection lasers increases with bias level. Unfortunately, injection lasers tend to exhibit stationary self-pulsations when they are dc biased to more than a few percent above threshold [7.85, 91, 93, 95]. The frequency of these self-pulsations has a range from 0.1 to a few GHz and coincides with the modulation resonance frequency for sinusoidal modulation. As the modulation depths can take values up to 80% [7.96], this effect is a severe limitation for high-frequency direct modulation of injection lasers. Several theoretical models have been proposed for a physical understanding of the self-pulsations.

Basov et al. [7.91, 97] supposed spatial inhomogeneities to be the reason for the self-pulsations. The influence of spatial inhomogeneities on the laser dynamics has been treated by the simple theoretical model of a laser divided into Sects. 1 and 2 (Fig. 7.17). The gain in the two sections can be controlled

separately by the injection currents I_1 and I_2. Both active regions are within the same Fabry–Perot resonator. To achieve laser action it is sufficient that only one of the sections exhibits optical gain. In the diode which is only biased in the lossy region a photon field in the resonator raises the electron level, whereas in the diode, which exhibits optical gain, the electron density is lowered by a photon field. Now if the absorbing section saturates faster than the amplifying one, there exists a region of photon number where the net optical amplification in the Fabry–Perot resonator increases with the photon number and the steady-state solution of the laser rate equations becomes unstable.

If r_{st1} and r_{st2} are the stimulated emission coefficients in Sects. 1 and 2, and γ is the ratio of the volume of Sect. 2 to that of Sect. 1, the condition of instability is

$$r_{st1}\frac{\partial r_{st1}}{\partial n_1}+\gamma r_{st2}\frac{\partial r_{st2}}{\partial n_2}<0. \tag{7.21}$$

By this model possible pulsations can be explained in all laser structures where the photon field can couple to lasing semiconductor regions with a band gap smaller than the photon energy.

Kobayashi has shown experimentally and theoretically that stationary pulsations can arise when two parallel lasers are optically coupled [7.98]. In the same way, self-pulsations could also be caused by the coupling of two filaments or two mode groups with different transverse mode structures. The theory of *Kobayashi* is on the basis of the rate equations and includes no mode locking phenomena, where the pulsation frequency is related to the difference of oscillating frequencies of interacting modes. Ordinary mode locking would yield spiking frequencies in the order of 10^{11} Hz. Therefore second-order mode locking has been proposed for injection lasers [7.85, 92, 99]. Although [7.100] brings experimental evidence for second-order mode locking, the measured pulsation behavior of lasers with a narrow emission spectrum [7.94] can rather be explained by the theory of *Basov*. We think that the Q switching, proposed by *Basov* is the main reason for spontaneous self-pulsing phenomena. These phenomena are surely influenced and possibly also enhanced by mode or filament interactions.

We have measured the microwave spectrum of the stationary optical output pulsations of dc operated low-mesa-stripe geometry DHS GaAs injection lasers. Figure 7.18 shows the typical decrease of the rf bandwidth of the output pulsations and the increase of the pulsation frequency and amplitude with increasing injection current. Generally we observed that an abrupt change in the self-pulsation frequency is always accompanied by a change in the filamentary structure of the near-field intensity distribution [7.95].

An emission spectrum without and with (Fig. 7.19) self-pulsations is shown for the same laser at different injection levels. Self-pulsations cause a broadening of the spectral envelope of the longitudinal modes and also a broadening of

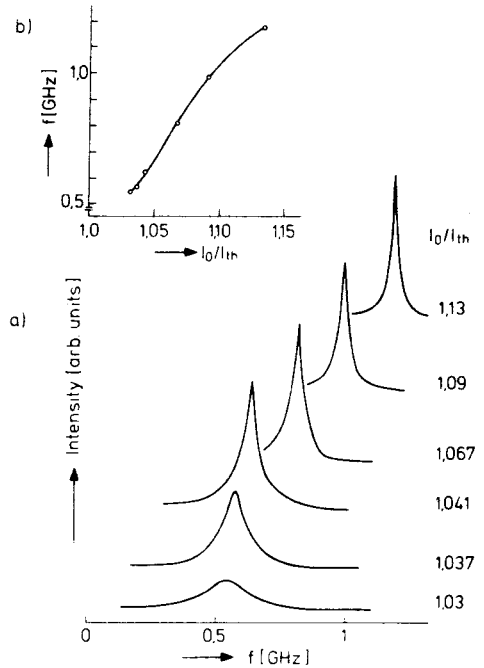

Fig. 7.18. (**a**) Frequency spectrum of the self-pulsations of a cw operated low-mesa-stripe GaAs/GaAlAs laser for different injection currents; (**b**) fluctuation frequency as a function of the normalized injection current I_0 I_{th}

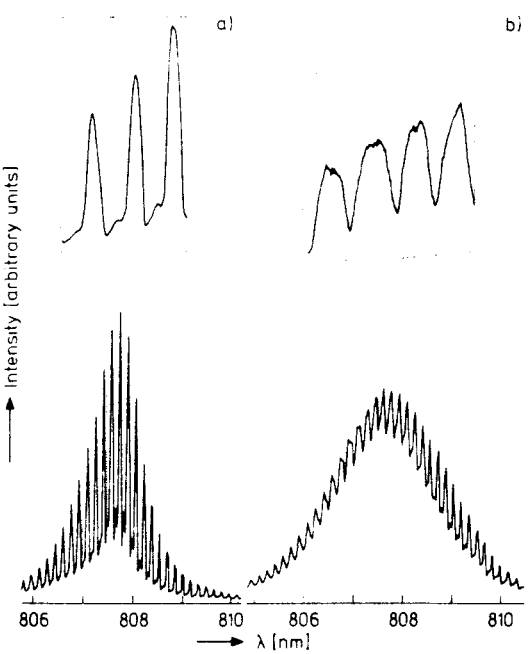

Fig. 7.19a, b. Longitudinal-mode spectra of a cw operated low-mesa-stripe GaAs GaAlAs laser: (**a**) laser operation without self-pulsations (I_0 = 214 mA); (**b**) laser operation with self-pulsations (I_0 = 283 mA)

the individual modes as can be obviously seen from the intersections in Fig. 7.19. The linewidth widens by a factor of two.

The broadening of the spectral lines can be explained in the following way. The self-pulsations cause an oscillation of the electron density and therewith also an oscillation of the refractive index in the active region and a corresponding oscillation in the wavelength shift. In the time averaged measurement this effect shows a spectral broadening. In spontaneously pulsating injection lasers the spectral broadening of the emission spectrum is the same as in the case of direct modulated injection lasers.

A significant correlation between the occurrence of nonlinearities in the light output vs current characteristics (so-called kinks) and the repetitive self-pulsation has also been observed [7.95]. A typical example of that kind is shown in Fig. 7.20. Figure 7.20a shows the light output vs current characteristic of a laser, where the self-pulsations (Fig. 7.20b) just occur at the onset of the "kinks" (shaded areas in Fig. 7.20a). It is interesting to consider the related near-field distribution (Fig. 7.21). As long as the near field shifts to the right boundary a self-pulsation occurs. For larger currents the near-field shift stops and the stabilized near field also yields a nonpulsing light output.

Experiments of that kind suggest that the repetitive self-pulsations are related to the transverse near-field movement into possibly absorbing regions. Therefore the most probable explanation for these self-pulsations is a repetitive Q-switching process induced by saturable absorbing regions, as mentioned above.

7.7 Coupled Laser Structures

Optically coupled injection lasers exhibit very interesting modulation and spectral properties. Depending on the strength of coupling quite different effects can be observed.

Strong optical coupling is achieved when both laser systems are within the same Bragg resonator or very close by aligned end to end [7.21, 97, 101]. We have discussed such a system in the preceding section. For inhomogeneous excitation there also exist points of operation where such junctions exhibit a bistable switching behavior. Applications can be seen for pulse shaping and optoelectronic logic AND gates.

Another promising application of optically coupled injection lasers is to improve the modulation performance of injection lasers. It has been shown theoretically and experimentally, that the modulation bandwidth of an injection laser can be increased by injection of a coherent light signal into one of its oscillating modes [7.102–109]. In section 7.3, we have shown that a high initial photon number in the oscillating modes causes a strong reduction of the relaxation oscillations. By injection of a coherent light signal into one oscillating mode of an injection laser, this strong reduction occurs without

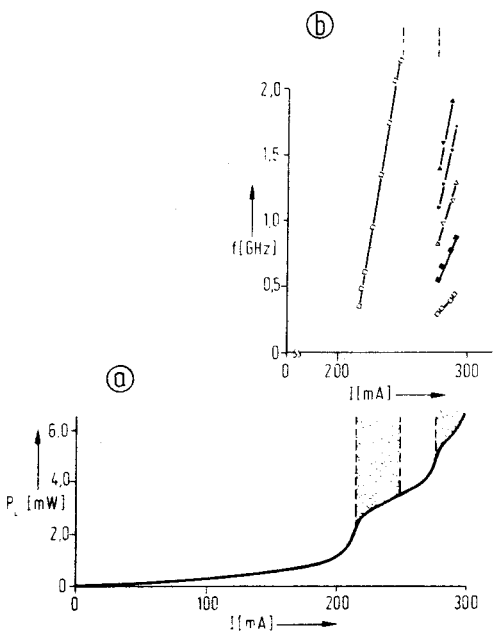

Fig. 7.20a, b. Light output vs current, and microwave frequency vs current characteristic of a proton-implanted laser

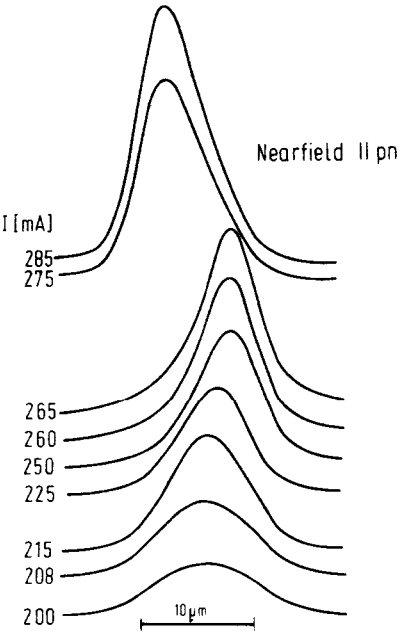

Fig. 7.21. Near-field distribution along the junction plane

multimode operation. Figure 7.22 shows the experimentally observed optical response of an injection laser to a step current pulse [7.108]. The computer simulation of a 2 Gbit s direct pulse code modulation of a multimode injection laser has shown that by coherent light injection not only the pattern effects are eliminated but also the nonirradiated modes are suppressed [7.104] (Fig. 7.23). The suppression of the nonirradiated modes results from the reduction of the electron density and the associated gain caused by the light injection. Practically, coherent light injection at the center wavelength of a mode is impossible and there is always a detuning between the wavelength of the injected radiation and the wavelength of the free-running laser mode. The locking range for synchronization to the wavelength of the injected radiation is proportional to the amplitude ratio of injected radiation and radiation produced in the laser and inversely proportional to the laser length [7.107–109]. For an amplitude ratio of 10^{-2} a locking range of more than 0.1 Å can be achieved [7.108, 109]. If two lasers with different longitudinal mode spacing are coupled, by appropriate choice of the laser parameters there always exists one or more pairs of modes with sufficiently close wavelengths to insure locking [7.107, 110].

Figure 7.24 shows the small-signal modulation depths vs modulation frequency characteristics with and without coherent light injection [7.109]. The

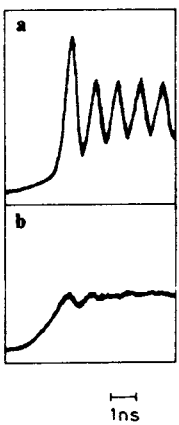

Fig. 7.22a, b. Response of an injection laser to a step current pulse with an amplitude approximately 3% above threshold without (**a**) and with (**b**) coherent light injection

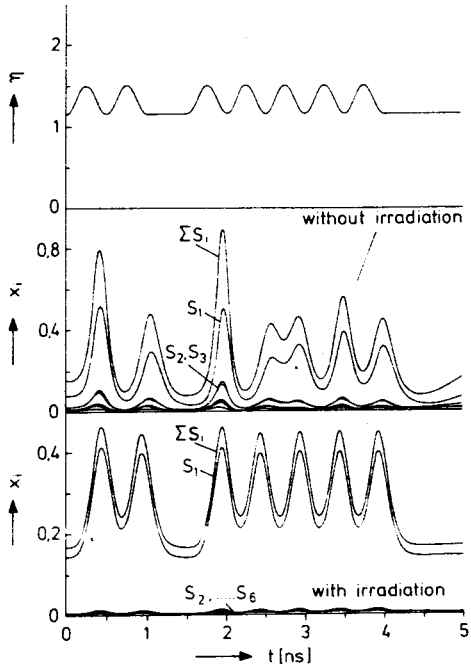

Fig. 7.23. Normalized photon numbers $x_i = S_i \tau_{sp} / V n_{th} \tau_{ph}$ and normalized modulation current $\eta = I / I_{th}$ as a function of time without and with coherent light injection

calculations with coherent light injection have been performed for different detuning $\Delta\lambda$ between the wavelength of the injected radiation and the free-running wavelength of the laser mode. When the detuning is smaller than the locking range, the resonance in the modulation characteristics vanishes. Figure 7.25 shows the large-signal response to a step pulse which changes I/I_{th} from 0.9 to 1.1 at the time $t=0$ [7.109]. With light injection the response is strongly damped within the whole locking range and exhibits no spiking response. For a detuning larger than the stationary locking range the frequency locking breaks down and the laser produces strong spiking oscillations. The frequency of these spiking oscillations is identical with the difference between the frequencies of the free-running mode and the incident radiation. This oscillation, induced by coherent light injection has also been experimentally observed [7.111].

7.8 Outlook

Although stripe-geometry DHS GaAs injection lasers under certain experimental conditions can be modulated up into the GHz region there are still problems

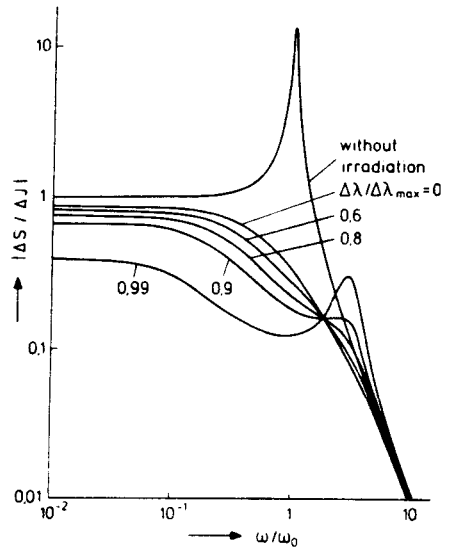

Fig. 7.24. Small-signal modulation depths vs modulation frequency characteristic with and without coherent irradiation for different ratios of the wavelength detuning range $\Delta\lambda$ to the wavelength locking range $\Delta\lambda_{max}$ ($\tau_{sp}/\tau_{ph}=10^3$, $l=3$, $\eta_0=1.1$)

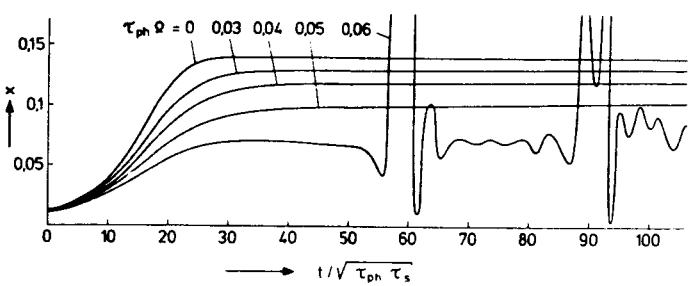

Fig. 7.25. Large-signal response to a step current pulse with coherent irradiation. Ω is the angular frequency difference between the free running mode and the injection radiation. The light injection intensity corresponds to a maximum locking range $\Omega\tau_{ph}=0.05$ ($\tau_{sp}/\tau_{ph}=10^3$, $l=3$)

to be solved for practical application. The self-pulsations can possibly be eliminated when laser structures can be developed where the optical field does not reach into absorbing regions with a band gap smaller than the photon energy.

Since the multimode emission structure is caused by spatial hole burning and the hole burning is intensified by a low minority carrier mobility, undoped active layers with a very good crystal perfection should be used. Another possibility to obtain a stable longitudinal single-mode output is the distributed feedback injection laser [7.112].

Theoretical investigations yield for distributed feedback injection lasers the same modulation behavior as for Fabry–Perot type monomode lasers [7.113]. Single longitudinal mode emission has also been reported for transverse-junction-stripe lasers [7.114, 72].

Coherent light injection will result in a considerable improvement in the high-frequency modulation behavior. Possibly the future development in integrated optics [7.115] will make monolithic integrated coupled laser structures feasible for technical applications.

Injection lasers which show a stable fundamental mode lasing operation are becoming more and more attractive as analogue transmitters in optical communication systems. Lasers exhibiting a good linearity between the light output and the injection current exhibit only little higher-order harmonic distortion. BH lasers (see Fig. 7.10g) show a second-order harmonic distortion of as low as about -50 dB, as reported in [7.116]. Stripe-geometry lasers with very narrow stripes as, for example, the *V*-groove laser (Fig. 7.10d) may also exhibit low harmonic distortions. In our laboratory, preliminary measurements showed a second-order distortion of -50 dB with a modulation of 1 mW peak-to-power light power, coupled into a fiber, for modulation frequencies up to about 100 MHz.

Today GaAs DHS injection lasers with stripe geometry are the most developed fiber optical transmitters. Increasing effort is undertaken in development of laser materials emitting at wavelengths around 1.2 to 1.3 μm since the fiber material dispersion vanishes there [7.117] (see Chap. 2). In this case, the spectral emission bandwidth of the laser does influence the transmission bandwidth of the optical fiber channels only by a second-order effect [7.118]. With InP/GaInAsP injection lasers of 1.1 to 1.3 μm emission wavelength cw lifetimes of 3500 hrs have been reported [7.14, 15].

Acknowledgment. The authors are indebted to F.-J. Berlec for assistance in performing the measurements and to H. Gottsmann, K. Wölk, and P. Marschall for the fabrication of the lasers investigated. This work has been sponsored by the "Bundesministerium für Forschung und Technologie". The authors alone are responsible for the content of the paper.

List of Symbols

a	Amplitude factor
c	Velocity of light in vacuum
d	Thickness of active layer
D	Diffusion constant [$cm^2 s^{-1}$]
D_n	Electron diffusion constant [$cm^2 s^{-1}$]
e_0	Absolute electron charge
E_i	Photon energy of ith mode
f	Frequency of self-pulsation
g	Gain of lasing mode
$\hbar$	Planck's constant
I	Injection current
I_{th}	Threshold injection current

I_0	dc bias current
I_p	Pulse current
$\tilde{I}_0(a)$	Modified Bessel function
J	Injection current density [$A\,cm^{-2}$]
J_{th}	Threshold current density [$A\,cm^{-2}$]
k	Boltzmann's constant, also wave number
L	Laser cavity length
L_n	Electron diffusion length
n	Electron density
n_{th}	Threshold electron density
$\bar{n}$	Index of refraction
$\bar{n}'$	Effective index of refraction
P_L	Light-output power per laser mirror
r_{sp}	Spontaneous emission rate per unit of volume and unit of photon energy E_i
r_{st}	Stimulated emission rate per unit of volume and unit of photon energy E_i
R_i	Reflectivity of end mirrors for the ith mode
R_{sp}	Total spontaneous emission rate
S	Photon number
S_i	Photon number in the ith mode
t	Time
t_d	Inital delay time
T	Absolute temperature
V	Active volume
x	Coordinate; normalized photon number
z	Normalized electron density
α	Spontaneous emission coefficient
α_i'	Internal optical loss per unit length
β	Damping parameter
γ	Volume ratio
Γ	Photon confinement factor
η	Normalized injection current
$\varkappa$	Internal quantum efficiency
λ	Emission wavelength
$\Delta\lambda$	Wavelength separation of neighboring longitudinal modes; wavelength detuning
Δ	Half-width of the stimulated emission
μ_n	Electron mobility
τ_{sp}	Spontaneous electron lifetime
τ_{ph}	Photon lifetime
φ_i	Normalized complex photon amplitude function
$\phi(E_i)$	Number of modes per unit volume and energy
ω	Angular frequency
Ω	Angular detuning frequency

References

7.1 G. Arnold, P. Russer: Appl. Phys. **14**, 255 (1977)
7.2 M. Boerner: Wiss. Ber. AEG-Telefunken **44**, 41 (1971)
M. Boerner, S. Maslowski: Proc. IEEE **123**, 627 (1976)
7.3 E. Weidel: Electron. Lett. **11**, 436 (1975)
7.4 D. Gloge: Appl. Opt. **10**, 2442 (1971)
7.5 D. Gloge: Appl. Opt. **13**, 249 (1974)
7.6 R. L. Hartman, R. W. Dixon: Appl. Phys. Lett. **26**, 239 (1975)
7.7 H. Kressel: Proc. Opt. Fibre Transm. Conf. II, Williamsburg, Va. (1977)
H. Kressel, J. K. Butler: *Semiconductor Lasers and Heterojunction LEDs* (Academic Press, New York 1977)
7.8 R. L. Hartman, N. E. Schumaker, R. W. Dixon: Appl. Phys. Lett. **31**, 756 (1977)
7.9 C. H. Gooch: *GaAs Lasers* (Wiley Interscience, London 1969)
7.10 L. A. D'Asaro: J. Lumin. **7**, 310 (1973)
7.11 M. B. Panish, I. Hayashi: Appl. Solid State Sci. **4**, 236 (1974)
7.12 I. Hayashi: Appl. Phys. **5**, 25 (1974)
7.13 M. B. Panish: Proc. IEEE **64**, 1512 (1976)
7.14 J. H. Hsieh, J. A. Rossi, J. P. Donelly: Appl. Phys. Lett. **28**, 709 (1976)
7.15 J. H. Hsieh: Proc. AGARD Conf., London (1977) p. 35/1
7.16 T. Yamamoto, K. Sakai, S. Akiba: Jpn. J. Appl. Phys. **16**, 1699 (1977)
7.17 K. Oe, S. Ando, K. Sugiyama: Intern. Conf. Integrated Optics and Opt. Fiber Commun., Tokyo (1977) post deadline paper P5
7.18 T. Yamamoto, K. Sakai, S. Akiba, Y. Itaga, Y. Suematsu: Intern. Conf. Integrated Optics and Opt. Fiber Commun., Tokyo (1977) paper B2–3
7.19 K. Wakao, H. Morita, T. Kambagashi, K. Iga: Jpn. J. Appl. Phys. **16**, 2075 (1977)
7.20 E. Haken, H. Haken: Z. Phys. **176**, 421 (1963)
7.21 G. J. Laser: Solid-State Electron. **7**, 707 (1964)
7.22 J. Vilms, L. Wandinger, K. L. Klohn: IEEE J. QE-**2**, 80 (1966)
7.23 H. Haug: Z. Phys. **194**, 482 (1966)
7.24 H. Haug: Z. Phys. **200**, 57 (1967)
7.25 M. J. Adams, P. T. Landsberg: In Ref. 7.9, p. 5
7.26 H. Haug: Phys. Rev. **184**, 338 (1969)
7.27 M. J. Adams: Opto-Electron. **5**, 201 (1973)
7.28 H. Statz, C. L. Tang, J. M. Lavine: J. Appl. Phys. **35**, 2581 (1964)
7.29 H. Haug: Z. Phys. **195**, 74 (1966)
7.30 J. Buus, M. Danielsen, P. Jeppesen, F. Mengel, H. Moeskjaer, V. Ostoich: Proc. 2nd Europ. Conf. Opt. Commun., Paris (1976) p. 231
7.31 W. Streifer, R. D. Burnham, D. R. Scrifres: IEEE J. QE-**13**, 403 (1977)
7.32 G. Lasher, F. Stern: Phys. Rev. **133**, A553 (1964)
7.33 H. C. Casey, Jr., F. Stern: J. Appl. Phys. **47**, 631 (1976)
7.34 F. Marinelli: Solid-State Electron. **8**, 939 (1965)
7.35 T. H. Zachos, J. E. Ripper: IEEE J. QE-**5**, 29 (1969)
7.36 H. C. Casey, Jr., B. I. Miller, E. Pinkas: J. Appl. Phys. **44**, 1281 (1973)
7.37 S. N. Biswas, N. Kumar: Indian J. Pure Appl. Phys. **11**, 855 (1973)
7.38 J. C. Dyment, J. E. Ripper, T. P. Lee: J. Appl. Phys. **43**, 452 (1972)
7.39 J. Angerstein, D. Siemsen: Arch. Elektron. Übertragungstech. **30**, 477 (1976)
7.40 K. Konnerth, C. Lanza: Appl. Phys. Lett. **4**, 120 (1964)
7.41 R. Roldan: Appl. Phys. Lett. **11**, 346 (1967)
7.42 D. A. Kleinman: Bell Syst. Tech. J. **43**, 1505 (1964)
7.43 D. Röss: Z. Naturforsch. **19a**, 1169 (1964)
7.44 T. Ikegami, K. Kobayashi, Y. Suematsu: Electron. Commun. Jpn. **53-B**, 82 (1970)
7.45 P. M. Boers, M. T. Vlaardingerbrook, M. Danielsen: Electron. Lett. **11**, 206 (1975)
7.46 T. Ozeki, T. Ito: IEEE J. QE-**9**, 388 (1973)
7.47 T. Ozeki, T. Ito: IEEE J. QE-**9**, 1098 (1973)
7.48 T. P. Lee, R. M. Derosier: Proc. IEEE **62**, 1176 (1974)
7.49 W. Harth, D. Siemsen: Arch. Elektron. Übertragungstech. **30**, 343 (1976)

7.50 T.Kobayashi, S.Takahashi: Jpn. J. Appl. Phys. **15**, 2025 (1976)
7.51 M.Chown, A.R.Goodwin, D.F.Lovelace, G.H.B.Thompson, P.R.Selway: Electron. Lett. **9**, 34 (1973)
7.52 H.W.Thim, L.R.Dawson, J.V.Di Lorenzo, J.C.Dyment, C.J.Hwang, D.L.Rode: Intern. Solid-State Circuits Conf., Dig. of Tech. Papers (1973) p. 92
7.53 P.Russer, S.Schultz: Arch. Elektron. Übertragungstech. **27**, 193 (1973)
7.54 D.Schicketanz: Siemens Forsch. Entwicklungsber. **2**, 218 (1973)
7.55 H.Yanai, M.Yano, T.Kamiya: IEEE J. QE-**11**, 519 (1975)
7.56 J.Gruber, P.Marten, R.Petschacher, P.Russer: IEEE Trans. COM-**7**, 1088 (1978)
7.57 M.Danielsen: IEEE J. QE-**12**, 657 (1976)
7.58 T.Ikegami, Y.Suematsu: Electron. Commun. Jpn. **51**, 51 (1968)
7.59 T.Ikegami, Y.Suematsu: Proc. IEEE **55**, 122 (1967)
7.60 F.L.Paoli, J.E.Ripper: Proc. IEEE **58**, 1457 (1970)
7.61 T.Ikegami, Y.Suematsu: Electron. Commun. Jpn. **53-B**, 69 (1970)
7.62 W.Harth: Electron. Lett. **9**, 532 (1973)
7.63 W.Harth, D.Siemsen: Arch. Elektron Übertragungstech. **28**, 391 (1974)
7.64 P.Russer, H.Hillbrand, W.Harth: Electron. Lett. **11**, 87 (1975)
7.65 H.Grothe, W.Harth, P.Russer: Electron. Lett. **12**, 522 (1976)
7.66 P.Marschall, E.Schlosser, C.Wölk: Electron. Lett. **15**, 38 (1979)
7.67 O.Nakada, N.Chinone, S.Nakamura, H.Nakashima, R.Ito: Jpn. J. Appl. Phys. **13**, 1485 (1974)
7.68 P.A.Kirkby, A.R.Goodwin, G.H.B.Thompson, P.R.Selway: IEEE J. QE-**13**, 705 (1977)
7.69 K.Aiki, M.Nakamura, T.Kuroda, J.Umeda, R.Ito, N.Chinone, M.Maeda: IEEE J. QE-**14**, 89 (1978)
7.70 K.Kobayashi, R.Lang, H.Yonezu, Y.Matsumoto, T.Shinohara, I.Sakuma, T.Suzuki, I.Hayashi: IEEE J. QE-**13**, 659 (1977)
7.71 M.Maeda, K.Nagano, I.Ikushima, M.Tanaka, K.Saito, R.Ito: Proc. 3rd Europ. Conf. Opt. Commun., NTG-Fachberichte Bd. **59**, 120 (1977)
7.72 H.Namizaki: Trans. Inst. Electron. Commun. Eng. Jpn. E-**59**, 8 (1976)
7.73 N.Chinone, K.Aiki, M.Nakamura, R.Ito: IEEE J. QE-**14**, 625 (1978)
7.74 Y.Suematsu, T.Hong, K.Furuya: Nachrichtent. Zeitschrift NTZ **31**, 127 (1978)
K.Furuya, Y.Suematsu, T.Hong: Appl. Opt. **17**, 1949 (1978)
7.75 T.Kobayashi, H.Kawaguchi, Y.Furukawa: Jpn. J. Appl. Phys. **16**, 601 (1977)
7.76 M.Nagano, K.Kasahara: IEEE J. QE-**13**, 632 (1977)
7.77 S.Iida, Y.Watanabe: Jpn. J. Appl. Phys. **13**, 1249 (1974)
7.78 J.E.Ripper, F.D.Nunes, N.B.Patel: Appl. Phys. Lett. **27**, 328 (1975)
7.79 B.W.Hakki: IEEE J. QE-**11**, 149 (1975)
7.80 T.L.Paoli: IEEE J. QE-**12**, 770 (1976)
7.81 C.H.Gooch: *Injection Electroluminescent Devices* (Wiley, London 1973) p. 138
7.82 T.L.Paoli, P.A.Barnes: Appl. Phys. Lett. **28**, 714 (1976)
7.83 R.W.Dixon, F.R.Nash, R.L.Hartman, R.T.Happlewhite: Appl. Phys. Lett. **29**, 372 (1976)
7.84 K.Kobayashi, R.Lang, H.Yonezu, J.Sakuma, I.Hayashi: Jpn. J. Appl. Phys. **16**, 207 (1977)
7.85 T.L.Paoli, J.E.Ripper: Phys. Rev. Lett. **22**, 1085 (1969)
7.86 T.Ikegami: Proc. 1st Europ. Conf. Opt. Commun. London (1975) p. 111
7.87 D.Siemsen, J.Angerstein: Electron. Lett. **12**, 432 (1976)
7.88 K.Petermann: Opt. Quantum Electron. **10**, 233 (1978)
7.89 P.R.Selway, A.R.Goodwin: Electron. Lett. **12**, 25 (1976)
7.90 W.Freude: Arch. Elektron. Übertragungstech. **32**, 105 (1978)
7.91 N.G.Basov, V.N.Morozov, V.V.Nikitin, A.S.Semenov: Sov. Phys. Semicond. **1**, 1305 (1968)
7.92 T.P.Lee, R.Roldan: IEEE J. QE-**5**, 551 (1969)
7.93 T.L.Paoli, J.E.Ripper: Appl. Phys. Lett. **18**, 466 (1971)
7.94 N.Chinone, R.Ito: Jpn. J. Appl. Phys. **13**, 575 (1974)
7.95 G.Arnold, K.Petermann: Self-pulsing phenomena in injection lasers. Opt. Quant. Electron. **10**, 311 (1978)
7.96 T.L.Paoli: IEEE J. QE-**13**, 351 (1977)
7.97 N.G.Basov: IEEE J. QE-**4**, 855 (1968)
7.98 K.Kobayashi: IEEE J. QE-**9**, 449 (1973)
7.99 H.-G.Wöhrstein, H.Haken: IEEE J. QE-**9**, 318 (1973)

7.100 J.E.Ripper, T.L.Paoli: IEEE J. QE-**8**, 74 (1972)
7.101 A.B.Fowler: J. Appl. Phys. **35**, 2275 (1964)
7.102 P.Russer: Arch. Electron. Übertragungstech. **29**, 231 (1975)
7.103 P.Russer: Laser 75 Optoelectron. Conf. Proc., München (1975) p. 161
7.104 H.Hillbrand, P.Russer: Electron. Lett. **11**, 372 (1975)
7.105 R.Lang, K.Kobayashi: IEEE J. QE-**11**, 60D (1975)
7.106 K.Kobayashi, R.Lang, K.Minemura: Proc. 1st Europ. Conf. Opt. Commun., London (1975) p. 138
7.107 R.Lang, K.Kobayashi: IEEE J. wE-**12**, 194 (1976)
7.108 P.Russer, G.Arnold, K.Petermann: High-speed modulation of DHS lasers in the case of coherent light injection. Proc. 3rd Europ. Conf. Opt. Commun. München, 1977
7.109 G.Arnold, K.Petermann, P.Russer, F.-J.Berlec: Arch. Elektron. Übertragungstech. **32**, 129 (1978)
7.110 R.Salathé, C.Voumard, H.Weber: Phys. Status Solidi (a) **23**, 675 (1974)
7.111 J.-I.Nishizawa, K.Ishida: IEEE J. QE-**11**, 515 (1975)
7.112 M.Nakamura, K.Aiki, J.Umeda, A.Yariv: Appl. Phys. Lett. **27**, 403 (1975)
7.113 S.R.Chinn: Opt. Commun. **19**, 208 (1976)
7.114 H.Namizaki: IEEE J. QE-**11**, 427 (1975)
7.115 T.Tamir(ed.): *Integrated Optics*, Topics in Applied Physics, Vol. 7 (Springer, Berlin, Heidelberg, New York 1975)
7.116 K.Nagano, M.Maeda, K.Saito, M.Tanaka, R.Ito: Trans. IECE of Jpn. E-**61**, 441 (1978)
7.117 D.N.Payne, W.A.Gambling: Electron. Lett. **11**, 176 (1975)
7.118 F.P.Kapron: Electron. Lett. **13**, 96 (1977)

Additional References with Titles

S.M.Abbott, W.M.Muska, T.P.Lee, A.G.Dentai, C.A.Burrus: 1.1 Gbit/s pseudorandom pulse-code modulation of 1.27 μm wavelength cw InGaAsP/InP d.h. lasers. Electron. Lett. **14**, 349 (1978)
S.Akiba, K.Sakai, T.Yamamoto: Direct modulation of InGaAsP/InP double heterostructure lasers. Electron. Lett. **14**, 197 (1978)
C.Baack, G.Elze, B.Enning, G.Walf: Modulation behaviour in the gigabit range of several GaAlAs lasers. Frequenz **32**, 346 (1978)
J.A.Copeland: Semiconductor-laser self pulsing due to deep level traps. Electron. Lett. **14**, 809 (1978)
G.Deutsch, G.Lindner, K.Lübke, H.W.Thim: High-bit-rate pulse regeneration and modulation of injection lasers with a planar Gunn device. Electron. Lett. **15**, 285 (1979)
W.Freude: Monomode operation of direct modulated GaAlAs DHS injection lasers from 260 Mbit /s up to 1.4 Gbit/s. Arch. Elektron. Übertragungstech. **32**, 105 (1978)
O.Hirota, Y.Suematsu: Noise properties of injection lasers due to reflected waves. IEEE J. Quant. Electron. QE-**15**, 142 (1979)
T.-H.Hong, Y.Suematsu: Harmonic distortion of injection lasers. Trans. IECE Jpn. E **62**, 144 (1979)
D.Kato: High-quality broad-band optical communication by timedivision multiplexed pulse analog modulation: nonlinearity in diode lasers. IEEE J. QE-**14**, 343 (1978)
T.Ito, K.Nakagawa, K.Aida, K.Takemoto, K.Suto: Nonrepeatered 50 km transmission experiment using low-loss optical fibres. Electron. Lett. **14**, 520 (1978)
M.Ito, T.Kimura: Longitudinal mode competition in a pulse modulated AlGaAs DH semiconductor laser. IEEE J. QE-**15**, 542 (1979)
W.Lange: Intensity fluctuations of injection lasers operated with high frequency modulation. Electron. Lett. **14**, 7 (1978)
K.Nawata, S.Machida, T.Ito: An 800 Mbit/s optical transmission experiment using a single-mode fiber. IEEE J. QE-**14**, 98 (1978)
M.Saruwatari, K.Asatani, J.-I.Yamada, I.Hatakeyama, K.Sugiyama, T.Kimura: Low loss fibre transmission of high speed pulse signals at 1.29 μm wavelength. Electron. Lett. **14**, 187 (1978)
T.Yamamoto, K.Sakai, S.Akiba: Fast pulse behaviour of InGaAs/InP double-heterostructure lasers at 1.27 μm. Electron. Lett. **13**, 142 (1977)